Propagation of a Solute Wave in a Curved Vessel

G. PONTRELLI [1] and A. TATONE [2]

[1] *Istituto per le Applicazioni del Calcolo, CNR*
Viale del Policlinico 137, 00161 Roma, Italy
`g.pontrelli@iac.cnr.it`

[2] *DISAT, Facoltà di Ingegneria, Università dell'Aquila,*
67040 Monteluco di Roio (AQ), Italy
`tatone@ing.univaq.it`

Mass transport and diffusion processes of a substance dissolved in the blood are studied. A linearization procedure over the steady state solution is carried out and an asymptotic analysis is used to study the influence of a small curvature with respect to the straight tube. Numerical results show the characteristics of the long wave propagation and the role played by the curvature on the solute distribution.

Key words: *Wave propagation, solute dynamics, numerical methods.*

1. Introduction

Mass transfer and diffusion phenomena inside the arterial lumen and through the vascular wall are of great importance for physiological functions, such as oxygenation, nourishment of tissues and metabolic drainage processes. Some mathematical models coupling 3D flow and solute dynamics have been developed in recent years [1–4]. They are defined in a finite arterial segment of arbitrary shape, where an inflow solute distribution is provided [1, 2]. Some of them consider also absorption and exchange through the vascular tissues [3]. All these models provide the local concentration pattern and are useful to understand the relationship between the local flow pattern, the nourishing of arterial tissues and possible pathologies derived when such a process is altered [4].

It is known that geometrical effects, such as curvature, will strongly affect the flow pattern and consequently the concentration of gases and substances dissolved in the blood [5]. It is worth to investigate how, and to what extent, the geometry and the haemodynamic factors are responsible for anomalous accumulation and altered absorption of substances on the arterial wall, leading to atherosclerotic lesions and degenerative processes [6].

In the present paper, a perturbation approach is used to model the mass transport and diffusion process inside a straight or moderately curved artery, similarly to the work in [7]. It is described by the advection-diffusion equation and a Robin interface condition is imposed at the boundary to model a solute exchange through the wall, with the flow field given. For most substances such a process is convection dominated, due to a low diffusion coefficient [5]. Being interested in propagative phenomena, we consider the solute dynamics inside the vascular tissue negligible, and the so called *free-wall* model is used [4].

Induced by the periodicity of respiratory, hormonal and feeding acts, the concentration of a substance in blood is subject both to an oscillation in time and to a spatial variation along the vessel, sustained by the fluid motion [5, 6]. For example, the pulsatile insulin release in the blood stream is induced by the oscillation in glycolysis and generates a wave of period 5–10 min. [8]. In general, the wave period is strongly dependent on the substance considered. As a consequence, for any substance, we look for the propagation characteristics, in relation with the medium diffusivity and wall permeability properties. The aim of this study is to characterize the solute propagation in the blood flow and to provide the local distribution of concentration that can be affected by geometrical factors, such as the curvature.

The layout of this paper is as follows: in Sec. 2 the mathematical problem is stated in its general formulation as a convection-diffusion equation and its coupling with fluid dynamics is shown. For simplicity, the diffusivity and the wall permeability coefficients are assumed constants. Hence, a linearization procedure over a steady state solution is accomplished and a splitting of the concentration variable from the fluid dynamical field is achieved. A wave type solution in a torus is sought for the unsteady component (Sec. 3) and a perturbation method is used to separate the dominant component in a straight tube from the part due to a possible small curvature (Sec. 4). Finally, in Sec. 5 some numerical experiments show the characteristics of the wave propagation in a straight and in a bended artery and the influence of geometrical factors on the solute distribution.

2. The Advection-diffusion Problem

The motion of blood in a vessel is modelled by the flow of a newtonian viscous fluid in an elastic tube. Different substances are dissolved in blood, transported through the stream and possibly exchanged through the arterial wall [5, 6]. For simplicity, the presence of one solute only is considered and let us denote by c its concentration. Because of both diffusive and convective phenomena, c satisfies the following advection-diffusion equation [1]:

$$\frac{\partial c}{\partial t} + \mathbf{v} \cdot \nabla c - \mu \Delta c = 0 \tag{2.1}$$

with $\mathbf{v}$ the fluid velocity, $\mu > 0$ a diffusivity coefficient. A possible exchange of solute through the wall is expressed by:

$$(\mu \nabla c) \cdot \mathbf{n} + \sigma c = \sigma c_{\text{ext}} \tag{2.2}$$

where $\sigma \geq 0$ is the wall permeability and c_{ext} is a concentration external to the vessel (if the wall is impermeable, $\sigma = 0$). In the following, we will be interested in the concentration dynamics in the lumen only. Therefore the present model does not account for any possible external variations of concentration, and c_{ext} is considered constant. Strictly speaking, μ and σ do depend on the flow field and on the temperature [1, 2] but, for simplicity, let us assume them as constant. Due to the small value of μ, for most substances the problem is highly convection dominated in large arteries.

In principle, fluid and solute dynamics are coupled processes and influence reciprocally. However in this model the solute is regarded as a passive scalar: it is simply advected by the blood flow in the lumen, any feedback effect on the fluid viscosity and density being neglected. As a consequence, we split the flow from the solute dynamics: the fluid velocity $\mathbf{v}$ is computed beforehand, and Eqs. (2.1)–(2.2) are subsequently solved.

Problem (2.1)–(2.2) is usually defined in an arterial segment with proximal and distal boundary conditions assigned, together with an initial condition. By standard arguments for parabolic problems, it can be proved that, under appropriate regularity assumptions on the coefficients and on the velocity field, the above boundary value problem is mathematically well posed [4, 9]. However, since a special case will be studied here, the definition of proximal/distal boundary conditions will be again addressed in Sec. 3.

Let us decompose the variables $\mathbf{v}$ and c as sum of a steady state part (denoted by a bar) and an unsteady component (denoted by a circumflex

accent):

$$\mathbf{v} = \bar{\mathbf{v}} + \hat{\mathbf{v}}, \quad c = \bar{c} + \hat{c} \tag{2.3}$$

and let us assume the unsteady parts $\hat{\mathbf{v}}$ and $\hat{c}$ (and $\nabla\hat{\mathbf{v}}$ and $\nabla\hat{c}$ as well) are *small* enough with respect to the steady ones such that the nonlinear term $\mathbf{v} \cdot \nabla c$ in Eqs. (2.1) can be linearized as:

$$(\bar{\mathbf{v}} + \hat{\mathbf{v}}) \cdot (\nabla\bar{c} + \nabla\hat{c}) \approx \bar{\mathbf{v}} \cdot \nabla\bar{c} + \bar{\mathbf{v}} \cdot \nabla\hat{c} + \hat{\mathbf{v}} \cdot \nabla\bar{c} \tag{2.4}$$

neglecting the higher order terms. In other words, small fluctuations of velocity and concentration are superimposed to a steady solution.

It is easy to verify that:

$$\bar{c} = \begin{cases} c_{\text{ext}} & \text{if } \sigma \neq 0, \\ \text{const} & \text{if } \sigma = 0 \end{cases} \tag{2.5}$$

satisfies the following boundary value problem:

$$\bar{\mathbf{v}} \cdot \nabla\bar{c} - \mu\Delta\bar{c} = 0$$
$$\mu\nabla\bar{c} \cdot \mathbf{n} + \sigma\bar{c} = \sigma c_{\text{ext}} \quad \text{at the wall} \tag{2.6}$$

where $\bar{c}$ equals the constant value as in Eq. (2.5) at any boundary other than the wall. This corresponds to the fact that, for a time interval long enough, the solute pervades the whole tube and, in the limit, it reaches a uniform concentration.

3. Wave Solution

By Eqs. (2.4) and (2.6), the unsteady solution satisfies the following equation:

$$\frac{\partial\hat{c}}{\partial t} + \bar{\mathbf{v}} \cdot \nabla\hat{c} + \hat{\mathbf{v}} \cdot \nabla\bar{c} - \mu\Delta\hat{c} = 0 \tag{3.1}$$

with a homogeneous boundary condition at the wall:

$$\mu\nabla\hat{c} \cdot \mathbf{n} + \sigma\hat{c} = 0. \tag{3.2}$$

Because of Eq. (2.5), the homogeneous boundary value problem (3.1)–(3.2) depends only on the steady fluid velocity $\bar{\mathbf{v}}$ and is independent of the unsteady flow field $\hat{\mathbf{v}}$. This proves that the small wall deformation, which is demonstrated of much importance in vascular dynamics [7], is irrelevant in the solute motion.

We are going now to define a precise domain and a specific form for the solution of the problem (3.1)–(3.2). Let us consider a *long* tube of circular cross section of radius a, having the shape of a torus with small curvature $1/R$.

For the following analysis, it is convenient to work out the equations in a toroidal coordinate system (r, θ, ψ). The axial coordinate $z = R\theta$ is introduced to avoid degeneracy when $R \to \infty$ (straight tube).

The problem is now rewritten in nondimensional form by the following substitutions:

$$r \to \frac{r}{a}, \quad z \to \frac{z}{a}, \quad t \to \frac{Vt}{a}, \quad \mathbf{v} \to \frac{\mathbf{v}}{V}$$

where V is a characteristic velocity. Without loss of generality, the concentration is considered dimensionless.

Denoting by:

$$\text{Pe} = \frac{aV}{\mu} \quad \text{(Péclet number)}, \qquad \text{Sh} = \frac{a\sigma}{\mu} \quad \text{(Sherwood number)}$$

two characteristic numbers, the governing Eqs. (3.1)–(3.2) become:

$$\frac{\partial \hat{c}}{\partial t} + \bar{\mathbf{v}} \cdot \nabla \hat{c} - \frac{1}{\text{Pe}} \nabla^2 \hat{c} = 0,$$

$$\nabla \hat{c} \cdot \mathbf{n} + \text{Sh}\, \hat{c} = 0. \tag{3.3}$$

The physiological and metabolic functions of living beings are typically periodic and an intermittent release of substances (i.e. oxygen, hormones, nutrients, waste products) in the blood is carried out by several organs and glands. For example, respiratory and digestive acts have a period ranging, according to the species, from seconds to hours. It is realistic to assume that, for each substance, there exists a pulsatile source of solute concentration that, advected by the fluid, propagates downstream. As the blood flow is essentially unidirectional, the unsteady component $\hat{c}$ is sought in the form of an harmonic longitudinal travelling wave:

$$\hat{c} = \tilde{c}(r, \psi) e^{i(\omega t - kz)} \tag{3.4}$$

with ω a nondimensional circular frequency $(\omega \to \omega a/V)$ and k the nondimensional wave number $(k \to ka)$. Consequently, the nondimensional wave speed is $\omega/\text{Re}(k)$ and the nondimensional wavelength is $1/\text{Re}(k)$. Because of the explicit dependence on z and t in the waveform Eq. (3.4), neither proximal and distal boundary conditions, nor an initial condition are required.

For the following analysis, it is worth to express the amplitude of the wave (3.4) in terms of a *mass per unit length* defined by:

$$Q := \int\limits_0^1 \tilde{c}(r)r dr \qquad (3.5)$$

Concentration wave (3.4) has no direct relation with the pressure wave generated by the heart beat and transmitted by the fluid through the vessel distensibility. In physiological cases, ω is generally very low ($\omega \ll 1$).

4. Asymptotic Analysis

All arteries are affected by a small or moderate degree of curvature. A perturbation method is used to study the influence of a small curvature with respect to the straight case. As the curvature parameter $\varepsilon = a/R$ is assumed to be small ($\ll 1$), the amplitude in Eq. (3.4) is expanded as a power series of ε over an axisymmetric solution $c_0(r)$:

$$\tilde{c}(r, \psi) = c_0(r) + \varepsilon c_1(r, \psi) + \varepsilon^2 c_2(r, \psi) + \ldots \qquad (4.1)$$

The fluid steady velocity $\bar{\mathbf{v}}$ undergoes a similar expansion over $\bar{\mathbf{v}}_0$:

$$\bar{\mathbf{v}}(r, \psi) = \bar{\mathbf{v}}_0(r) + \varepsilon\bar{\mathbf{v}}_1(r, \psi) + \varepsilon^2\bar{\mathbf{v}}_2(r, \psi) + \ldots \qquad (4.2)$$

with $\bar{\mathbf{v}}_0$ is the Poiseuille velocity and $\bar{\mathbf{v}}_1$ is the first order velocity for a moderately curved tube [11]. Therefore one has:

$$\bar{\mathbf{v}}\cdot\nabla\tilde{c} = (\bar{\mathbf{v}}_0 + \varepsilon\bar{\mathbf{v}}_1)\cdot(\nabla c_0 + \varepsilon\nabla c_1) = \bar{\mathbf{v}}_0\cdot\nabla c_0 + \varepsilon(\bar{\mathbf{v}}_1\cdot\nabla c_0 + \bar{\mathbf{v}}_0\cdot\nabla c_1) + \varepsilon^2 \ldots \quad (4.3)$$

Expression (3.4) and expansions (4.1)–(4.3) are substituted in Eqs. (3.3), and terms of the same power of ε, up to the first order, are equated.

0-th order solution

The amplitude of concentration in a straight tube is governed by the following linear equation:

$$i\omega c_0 + \bar{\mathbf{v}}_0 \cdot \nabla c_0 - \frac{1}{\text{Pe}}\nabla^2 c_0 = 0. \qquad (4.4)$$

Letting $\omega_P = \omega\mathrm{Pe}$ (*scaled frequency*) and $k_P = k\mathrm{Pe}$ (*scaled wavenumber*), Eq. (4.4) is rewritten in scalar notations as:

$$\frac{d^2 c_0}{dr^2} + \frac{1}{r}\frac{dc_0}{dr} + i\left(k_P \bar{w}_0 - \omega_P\right) c_0 = 0 \qquad (4.5)$$

where all terms containing k^2 have been neglected, since large wavelengths are considered in the present application, and

$$\bar{w}_0(r) = 1 - r^2$$

is the Poiseuille axial velocity profile, nondimensionalized by scaling with V.

The boundary conditions associated with the Eq. (4.5) are:

$$\frac{dc_0}{dr} = 0 \qquad \text{at } r = 0 \quad \text{(symmetry condition)}, \qquad (4.6)$$

$$\frac{dc_0}{dr} + \mathrm{Sh}\, c_0 = 0 \qquad \text{at } r = 1. \qquad (4.7)$$

For a given frequency ω_P, the Sturm-Liouville eigenvalue problem (4.5)–(4.7) is solved to obtain the wave number k_P which corresponds to an admissible c-wave solution in a straight tube.

Through a variable transformation, we obtain the general integral of Eq. (4.5) written in terms of two constants A and B:

$$c_0(r) = \exp\left(-\frac{G}{2}r^2\right)\left[A\mathcal{L}\left(H - \frac{1}{2}, Gr^2\right) + B\mathcal{U}\left(\frac{1}{2} - H, 1, Gr^2\right)\right] r \quad (4.8)$$

with $\mathcal{L}$ the Laguerre function and $\mathcal{U}$ the Tricomi confluent hypergeometric function with complex argument [10] and with:

$$G = (ik_P)^{\frac{1}{2}}, \quad H = \frac{(ik_P)^{\frac{1}{2}}}{4}\left(1 - \frac{\omega_P}{k_P}\right).$$

A boundedness condition at $r = 0$ implies $B = 0$, and through the boundary condition (4.7), we obtain the *frequency equation*:

$$\left(\sqrt{k_P} + i^{\frac{3}{2}}\mathrm{Sh}\right)\mathcal{L}\left(H - \frac{1}{2}, G\right) + 2\sqrt{k_P}\mathcal{L}_g\left(H - \frac{3}{2}, 1, G\right) = 0 \qquad (4.9)$$

where $\mathcal{L}_g$ is the generalized Laguerre function. It gives the set of wavenumbers k_P correspondent to a given frequency ω_P. Finally, replacing in Eq. (4.8), one has:

$$c_0(r) = A\exp\left(-\frac{(ik_P)^{\frac{1}{2}}}{2}r^2\right)\mathcal{L}\left(\frac{(ik_P)^{\frac{1}{2}}}{4}\left(1 - \frac{\omega_P}{k_P}\right) - \frac{1}{2}, (ik_P)^{\frac{1}{2}}r^2\right) r.$$

$$(4.10)$$

The constant A is determined by using Eq. (3.5).

1st order solution

The correction due to a small curvature is described by the first order linear problem:

$$i\omega c_1 + \bar{\mathbf{v}}_0 \cdot \nabla c_1 - \frac{1}{\mathrm{Pe}} \nabla^2 c_1 = -\bar{\mathbf{v}}_1 \cdot \nabla c_0.$$

By letting:
$$c_1(r, \psi) = \check{c}_1(r) \sin \psi, \quad \check{c}_1 \to c_1 \qquad (4.11)$$

we obtain the non homogeneous problem:

$$\frac{\partial^2 c_1}{\partial r^2} + \frac{1}{r} \frac{\partial c_1}{\partial r} - \frac{c_1}{r^2} + i\left(k_P \bar{w}_0 - \omega_P\right) c_1$$

$$= ik_P \left(r\bar{w}_0 - w_d\right) c_0 + \left(\mathrm{Pe}\, u_d - 1\right) \frac{dc_0}{dr} \quad (4.12)$$

with the boundary conditions:

$$c_1 = 0 \quad \text{at } r = 0, \qquad (4.13)$$

$$\frac{dc_1}{dr} + \mathrm{Sh}\, c_1 = 0 \quad \text{at } r = 1. \qquad (4.14)$$

where u_d and w_d are respectively the nondimensional radial and the axial component of the steady flow in a curved tube [11]. Due to the antisymmetry of the first order solution c_1 (see Eq. (4.11)), the overall mass flux conservation of $c_0 + \varepsilon c_1$ in the half-section $(r, \psi) \in [0, 1] \times [-\pi/2, \pi/2]$ is guaranteed.

Note that the Péclet number appears at the right hand side of Eq. (4.12) as coefficient of u_d. The solution turns out to be strongly dependent on it, because it magnifies the role of secondary flow. Such effect exists as long as a transverse flow—induced by the curvature—is present, and grows with Pe.

5. Numerical Results and Discussion

The frequency Eq. (4.9) is solved numerically with a Newton type method by searching the complex roots k_P corresponding to a given ω_P. Because of the large wavelength, only the smallest root is selected. Results show that both wavelength and attenuation reduce with increasing ω_P and the effect of wall permeability is present only for small frequencies.

The curve connecting the pairs $(\omega_P, \omega_P/\mathrm{Re}(k_P))$ for $\omega_P \in [10^{-3}, 10^5]$ at varying Sh is shown in Fig. 1 (dispersion curve). It turns out that the wave
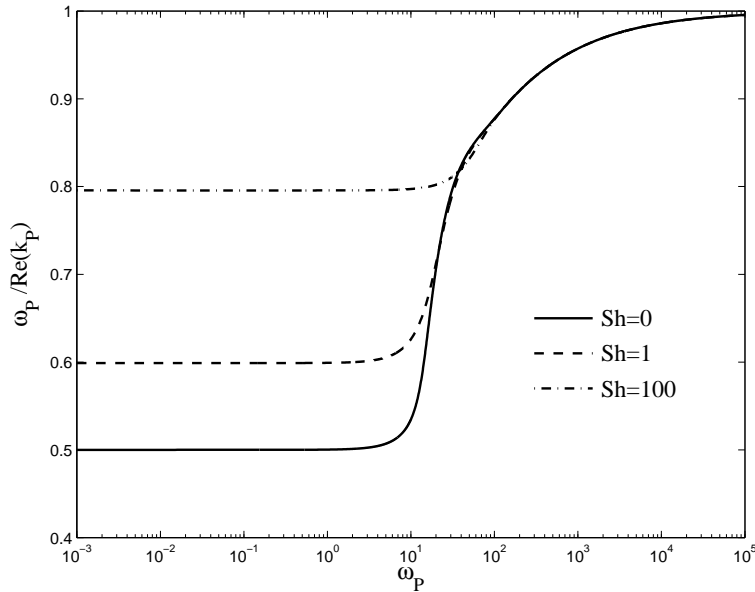
FIGURE 1. Dispersion curves for three different mass transfer coefficients Sh. The wave speed tends to the same asymptotic value for relatively high frequencies and exhibits a variation with Sh only at very low frequencies. In a range of typical frequencies ($10 \leq \omega_P \leq 100$) the speed undergoes a sudden raise.

speed tends to the value 1 (independent of Sh), for relatively large values of the frequency. On the other hand, at very small frequencies the wave speed is rapidly decreasing tending to a finite limit as $\omega_P \to 0$. Such limit is $1/2$ for Sh $= 0$ and increases with Sh. A critical frequency separates two regimes for each value of Sh: a layer where the velocity undergoes a sudden raise from a larger range where the velocity stays almost constant (Fig. 1).

The exact solution c_0 of the Eqs. (4.5)–(4.7) is given by Eq. (4.10). The boundary value problem (4.12)–(4.14) is then solved numerically with a collocation method using a cubic spline approximating function [12].

Once the analytical 0-th order solution is evaluated and the 1-st order problem solved numerically, the full wave solution is reassembled (see Eqs. (2.3), (3.4) and (4.1)) as:

$$c = \bar{c} + \tilde{c}e^{i(\omega t - kz)} = \bar{c} + (c_0 + \varepsilon c_1 \sin \psi)e^{i(\omega t - kz)}.$$

The physical problem depends on a number of parameters, each of them may vary in a quite wide range, and there is a variety of different limiting cases. In

the present work we will focus the attention on the influence of the solution c on the diffusivity—parametrized by Pe and on the wall permeability—parametrized by Sh. These two parameters are varied in a convenient interval to describe a number of substances dissolved in blood and different medium properties. Other parameters are fixed as:

$$a = 0.5 \, \text{cm}, \quad V = 24 \, \text{cm} \, \text{s}^{-1}, \quad Q = 0.01.$$

Concentration amplitudes c_0 for three typical values of ω_P are shown in Fig. 2. Approximately flat concentration profiles at low ω_P, are replaced by more oscillating fronts, with a possible undershooting, at higher ω_P. At relatively higher ω_P, the concentration flux occurs in the core of the vessel and is independent of Sh. The influence of curvature is small at low Pe, but becomes relevant at higher Pe, with a more pronounced oscillating profile (Fig. 3). At the high Péclet numbers under consideration ($\approx 10^5$), a noticeable difference with respect to a straight tube appears even for a curvature ratio small as $\varepsilon = 10^{-4}$. The first order solution c_1 is of few orders of magnitude higher than c_0, and their ratio grows with Pe. A significant result is the
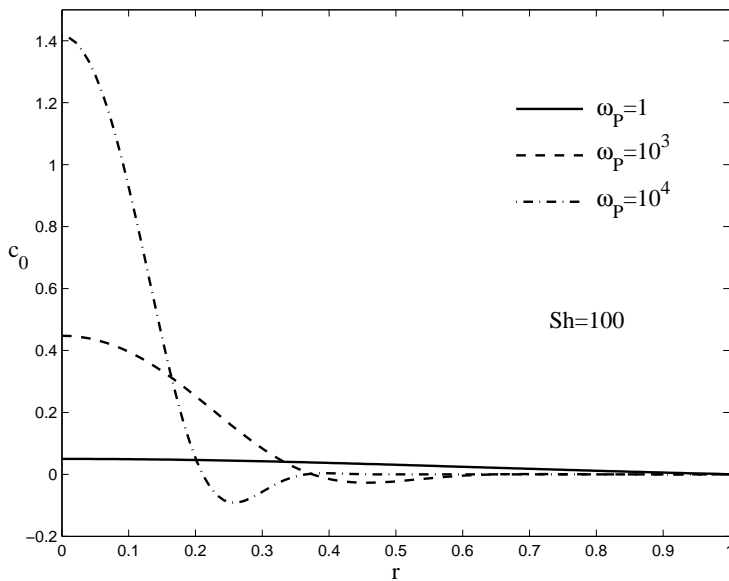

FIGURE 2. Concentration profiles along the horizontal half-diameter ($\psi = \pi/2$) of the cross section $z = 0$ at $t = 0$, for three values of ω_P. Differences with Sh are shown less pronounced and a core flux is evident at higher ω_P.
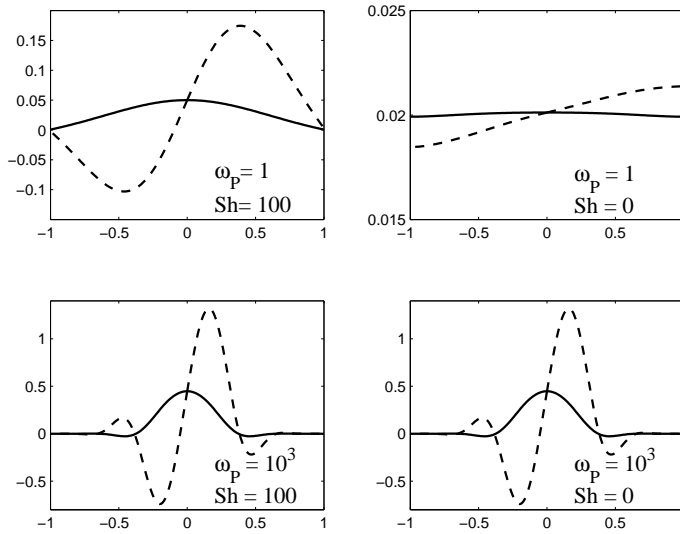
FIGURE 3. Concentration profiles along the horizontal diameter ($\psi = \pm\pi/2$) of the cross section $z = 0$ at $t = 0$ for Pe $= 10^5$. Plots highlight the combined effects of the wall permeability Sh (left-right) and of the wave frequency ω_P (top-bottom) in the case of a straight tube (continuous line) and of a slightly curved tube with $\varepsilon = 10^{-4}$ (dashed line). For such value of Pe, the solution is extremely sensitive to the curvature and, at low frequencies, even to Sh.

skewness of the c profiles: the maximum peak of concentration flux is shifted towards the outer bend and increases in magnitude. Consequently a wall flux reduction at the inner wall of the curvature is reported. This is in correlation with clinical observations of atherosclerotic lesions at the inner wall of arterial bends. The effect of the wall permeability on the concentration waveform is shown to be frequency dependent.

Acknowledgement

References

1. G. RAPPITSCH, K. PERKTOLD and E. PERNKOPF, *Numerical modelling of shear-dependent mass transfer in large arteries*, Int. J. Num. Meth. Fluids, **25** : 847–857, 1997.

2. G. Karner, K. Perktold, H.P. Zehentner and M. Prosi, *Mass transport in large arteries and through the arterial wall*, in: Intra and Extracorporeal Cardiovascular Fluid Dynamics, Adv. Fluid Mech., P. Verdonck and K. Perktold [Eds.] WIT press, Southampton, pp.209–247, 2000.

3. M. Prosi, K. Perktold, Z. Ding and M.H. Friedman, *Influence of curvature dynamics on pulsatile coronary artery flow in a realistic bifurcation model*, J. Biomech., **37** : 1767–1775, 2004.

4. A. Quarteroni, A. Veneziani and P. Zunino, *Mathematical and numerical modeling of solute dynamics in blood flow and arterial walls*, SIAM, J. Num. Anal., **39**(5) : 1488–1511, 2002.

5. J.A. Moore and C.R. Ethier, *Oxygen mass transfer calculations in large arteries*, J. Biomech. Eng., **119** : 469–475, 1997.

6. D.K. Stangeby and C.R. Ethier, *Computational analysis of coupled blood-wall arterial LDL transport*, ASME J. Biomech. Eng., **124** : 1–8, 2002.

7. G. Pontrelli and A. Tatone, *Wave propagation in a fluid flowing through a curved thin-walled elastic tube*, submitted to Europ. J. Mech., 2005.

8. M.G. Pedersen, R. Bertram and A. Sherman, *Intra- and inter-islet synchronization of metabolically driven insulin secretion*, Biophys. J. BioFAST, doi:10.1529/biophysj.104.055681, April 15, 2005.

9. A. Quarteroni and A. Valli, *Numerical approximation of partial differential equations*, Springer Series in Comp. Math. 23, Springer-Verlag, Berlin, 1997.

10. M. Abramowitz and I.A. Stegun [eds.], *Handbook of mathematical functions*, Washington DC, National Bureau of Standards, 1972.

11. W.R. Dean, *Note on the motion of fluid in a curved pipe*, Phil. Mag., **4** : 208–223, 1927.

12. J.D. Pryce, *Numerical solution of Sturm-Liouville problems*, Monographs on Numerical Analysis, Oxford University Press, Oxford, 1993.

———◇———